Electronic Supplementary Material (ESI) for Journal of Materials Chemistry

Electronic Supplementary Information (ESI)

Antioxidant activity of freestanding metal nanoparticles, *ex-situ* estimation of the stability of metal nanoparticles, and microscopic characterization of metal nanoparticles and silica support

Panagiotis Trogadas[a], Javier Parrondo[a], Federico Mijangos[b] and Vijay Ramani[*,a]

[a]Illinois Institute of Technology, Department of Chemical and Biological Engineering, Chicago, IL 60616

[b]University of the Basque Country, Department of Chemical Engineering, Leioa, Vizcaya 48940 (Spain)

Email: ramani@iit.edu; Tel: +1 312 567 3064

Antioxidant activity of metal nanoparticles

The capacity of metal nanoparticles to catalyze the decomposition of free radicals was determined *ex-situ* by their ability to reduce the concentration of the stable free radical 1,1-diphenyl-2-picrylhydrazyl (DPPH)[1-3]. The *ex-situ* experiments with DPPH were performed primarily as a simple screening test to check if the metal nanoparticles synthesized had any demonstrable antioxidant activity. 0.075 mmol DPPH was dissolved in 250mL of 80% vol ethanol-20% vol acetate buffer (0.1M, pH=5.4). An appropriate amount of 0.5wt% solution (stock solution in toluene) of the metal nanoparticles was dispersed in 50mL ethanol to obtain a suspension with a concentration of 10 mg/L. Then, 1mL of metal suspension (Au, Pd, Pt or Ag) was added to 2mL DPPH solution in a test tube. The test tube was heated to 80ºC in a thermostatic bath to increase the rate of reaction; the reaction was stopped after 30 min by cooling down the mixture in an ice bath. When the DPPH radical is scavenged by an antioxidant (metal nanoparticles), it transforms to 1,1-diphenyl-2-picrylhydrazyne (DPPH-H). As part of this transformation, the color of the solution turns from purple to yellow. The extent of the transformation (i.e. radical scavenging) was quantified by the decay in absorbance at 523nm over the duration of the test[4]. The concentration of free radicals was calculated with a calibration curve prepared dissolving the DPPH using the same conditions employed during the reaction. The UV-VIS absorbance data obtained is shown in Table S1 and the calculated rate of decomposition of DPPH is shown in Figure S1. In the presence of Ag nanoparticles, the UV-vis signal was identical to the baseline signal, suggesting that the silver nanoparticles had no impact in lowering the concentration of DPPH free radical. A 20%-25% decrease in UV-vis absorbance was observed when Au or Pd nanoparticles were immersed in the solution, although a greater decrease was

observed for Pt nanoparticles. Pt nanoparticles demonstrated the highest activity against DPPH radicals as a 50% decrease in UV-vis absorbance was achieved (Table S1) and almost double the rate of reaction was obtained when compared with Pd and Au nanoparticles (Figure S1). These preliminary screening results suggested that Au, Pt and Pd nanoparticles did have radical scavenging ability, even though their measured scavenging ability against DPPH radical cannot be a direct predictor of their efficacy in a fuel cell membrane as the testing environment varies considerably [from DPPH radical in solution (*ex-situ*) to hydroxyl radicals in an acidic Nafion® membrane (*in-situ*)].

Table S1. Scavenging activity of metal nanoparticles quantified by UV-vis spectroscopy

Sample	**Absorbance at 523nm after 30 min at 80°C**
Control	0.140
Pd nanoparticles	0.108
Ag nanoparticles	0.135
Pt nanoparticles	0.067
Au nanoparticles	0.112

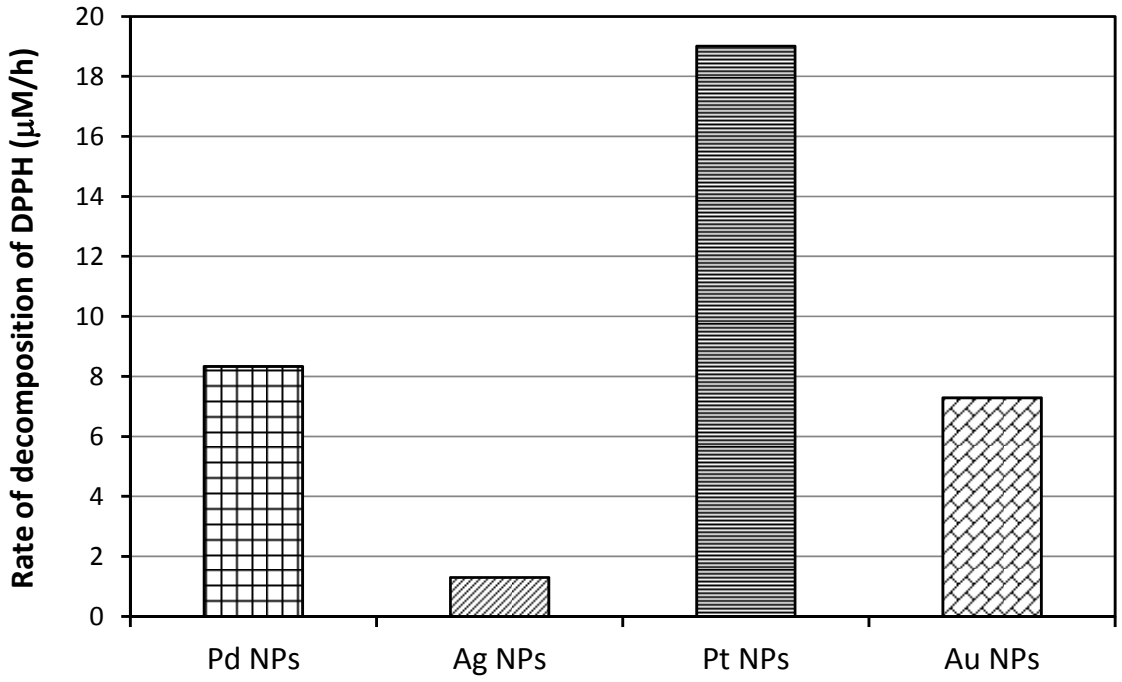

Figure S1. Rate of reaction for the decomposition of DPPH catalyzed by metal scavengers

The scavenging activity of metal nanoparticles against the DPPH free radical was also established by using electronic paramagnetic resonance (EPR) also known as electron spin resonance (ESR). The samples were prepared and treated as described above but the DPPH free radical was detected using electron spin resonance (ESR) spectroscopy. When the DPPH radical is scavenged by an antioxidant, it transforms to 1,1-diphenyl-2-picrylhydrazyne (DPPH-H). The extent of the transformation (i.e. radical scavenging) was be quantified by the decay in ESR signal.

X-band EPR measurements were carried out on a Bruker ELEXSYS 500 spectrometer with a maximum available microwave power of 200 mW and equipped with a super-high-Q resonator ER-4123-SHQ. The spectra were recorded at room temperature with the ER-160-FC-Q aqueous solution cell using a typical modulation amplitude of 0.1 mT at a frequency

of 100 kHz. The magnetic field was calibrated by a NMR probe and the frequency inside the cavity was determined with an integrated MW-frequency counter. The experimental conditions used for operating the instrument and the method used for the interpretation of the obtained spectra were adapted from the work of Krzystek and coworkers[5]. The ESR spectra are shown in Fig. S2.

In the presence of Ag nanoparticles, the ESR signal was identical to the baseline signal, proving as discussed earlier that the silver nanoparticles did not exhibit free radical scavenging activity. Gold showed some quenching of ESR signal and the highest decrease was observed in the case of Pt nanoparticles. These preliminary screening results using ESR confirmed the results previously obtained with the DPPH radical using UV-VIS spectroscopy.

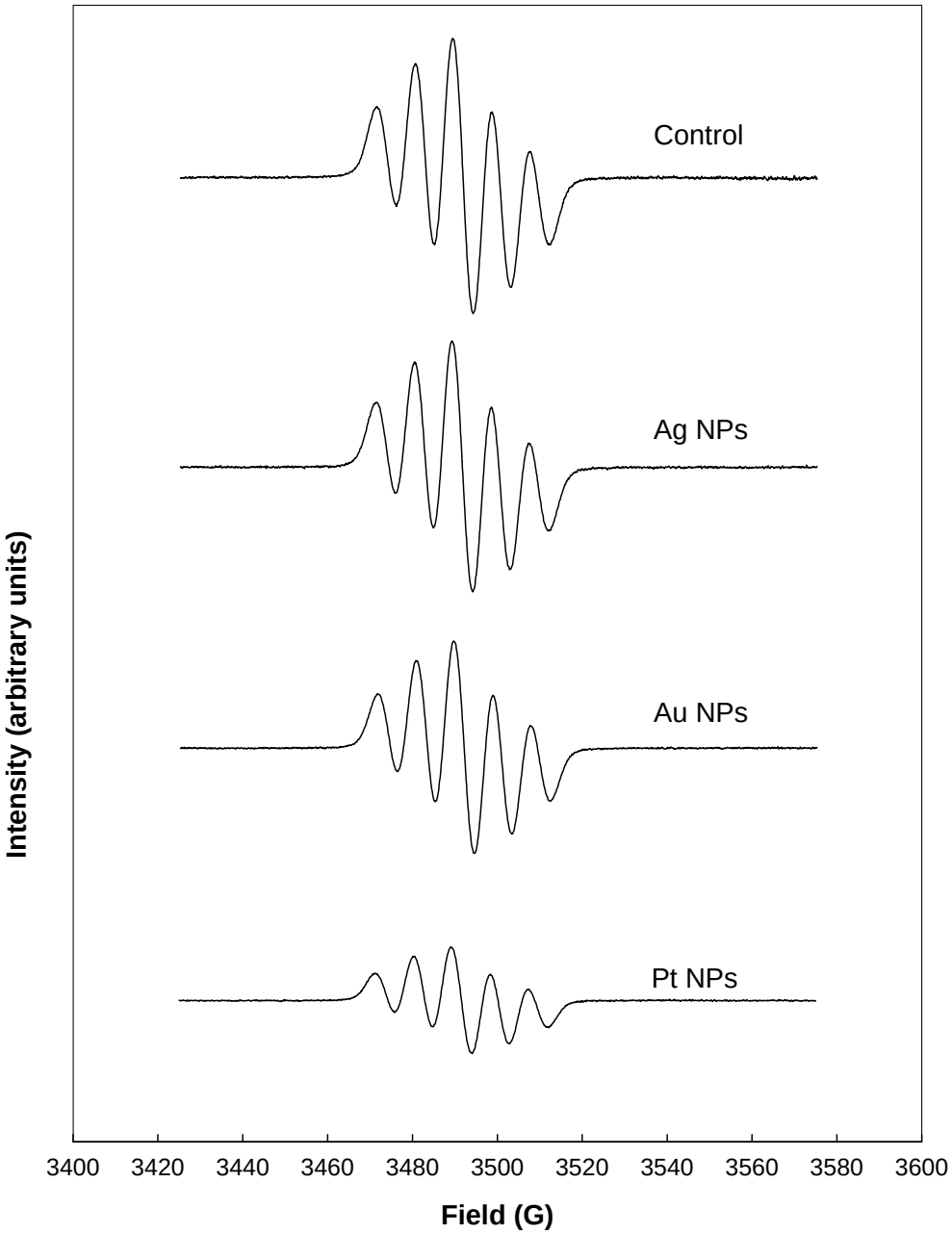

Figure S2. ESR spectra of DPPH free radical after catalyzed decomposition in the presence of metal nanoparticles. Reaction performed at 80ºC for 60 minutes. Reaction medium: 3 mg/L of metal nanoparticles, 0.2 mM DPPH, ethanol/acetate (85/15) buffer, pH=5.4.

***Ex-situ* estimation of stability of metal nanoparticles**

A simple experimental procedure was adopted to examine whether the added metal nanoparticles were oxidized to metal ions during fuel cell operation and then participated in Fenton-like reactions to generate harmful free radicals by the catalytic decomposition of hydrogen peroxide. In addition to antioxidant activity, one must consider the propensity of the metal nanoparticles and especially their ions to facilitate the production of free radicals from hydrogen peroxide. This propensity is largest for silver[6, 7]. Pt, Pd and Au nanoparticles also dissolve at high potentials in acidic media. The metal ions formed by dissolution can augment the production of hydroxyl radicals[8] thereby resulting in higher total FER values.

Recast Nafion® and composite Nafion® membrane samples were extracted from the tested MEAs by carefully removing the catalyst layers. The samples were trimmed to ensure roughly equal dimensions and exactly equal weights, washed with DI water, and dried overnight at 60^{o}C. They were then immersed in 30 ml of H_2O_2 solution (3wt%; Sigma Aldrich) for 24 hours. The fluoride ion concentrations in the H_2O_2 solution were measured using a fluoride ion selective electrode (Denver instruments) that was freshly calibrated before each measurement.

The results of the test are shown in Figure S3. There was no significant difference in the concentration of fluoride ions in test solutions containing composite membranes (with added metal nanoparticles) when compared to the test solutions containing the Nafion® control. This result suggested that the metal nanoparticles did not contribute to Fenton-type reactions that generate free radicals from hydrogen peroxide present within the PEM.

The stability of metal nanoparticles was not surprising considering the fact that much of the PEM cross-section was maintained at anode potential, wherein dissolution is not thermodynamically favored. For the small portion of the membrane (close to the cathode) where dissolution is indeed favored, we hypothesize that the metal ions generated were immediately exchanged with neighboring protons (leading to lowered conductivity as discussed previously) and that in this state, the ions were not active as Fenton catalysts.

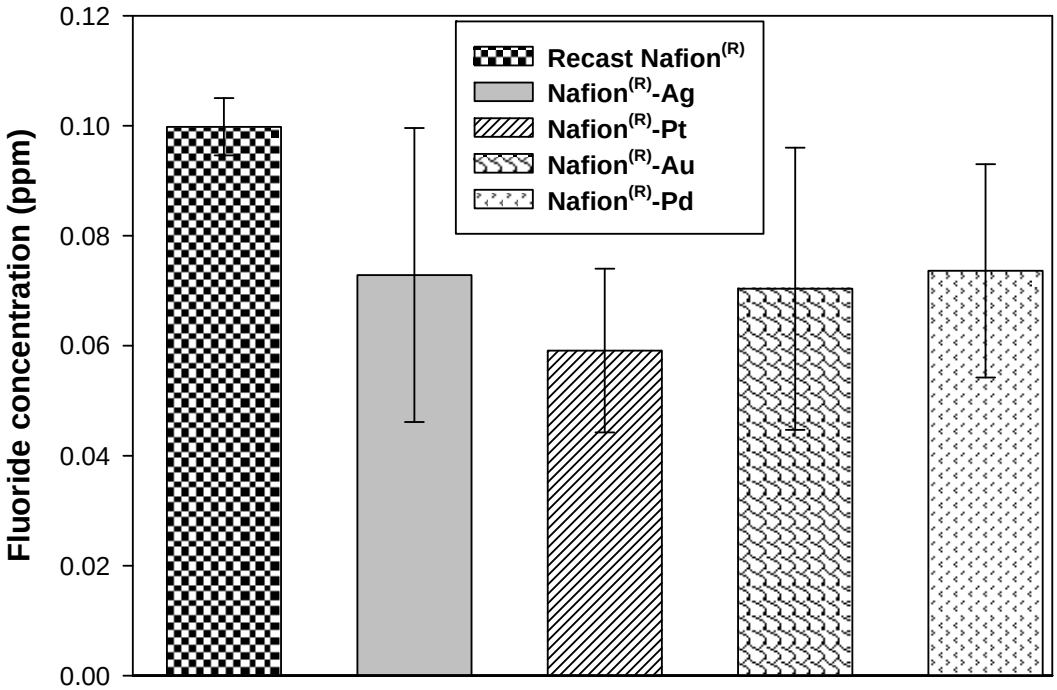

Figure S3. Fenton test to study the stability of metal nanoparticles (*ex-situ*)

Even so, the case for further optimizing supported metal nanoparticles for degradation mitigation through particle size control and enhancement of metal loading on the support is very strong when one considers in detail the issue of dissolution of unsupported metal nanoparticles in direct contact with the electrolyte in conjunction with extremes of potential that are sometimes seen during fuel cell operation. According to Pourbaix diagrams[9],

platinum and gold metals are oxidized at potentials of approximately 1 V (vs. SHE) and 1.3 V (vs. SHE) respectively at pH value of 1 which resembles the acidic environment of a Nafion® membrane. Palladium and silver are oxidized to Pd^{2+} and Ag^{+} at much lower potentials, namely 0.8 V (vs. SHE) and 0.4 V (vs. SHE). As discussed in the section on proton conductivity, under normal fuel cell operating conditions, the potential distribution in the thickness dimension of the PEM is close to anode potential (0 V vs. SHE) for the most of its thickness and rises to the cathode potential (~ 0.6 - 1 V vs. SHE) in a region close to the cathode[10]. At such high potentials Ag and Pd nanoparticles will be oxidized close to the cathode, resulting in an increase in the concentration of metal ions and hence a lowering of proton conductivity (as observed).

Even Pt and Au nanoparticles, despite their relatively higher oxidation potentials at the electrolyte pH, are not completely safe. It has been documented that during PEFC start-up, the cell can experience potentials as high 1-2V vs. SHE at either electrode[11, 12]. Such high potentials would facilitate the oxidation of Pt and Au in addition to Pd and Ag metal nanoparticles in the vicinity of the electrodes, potentially resulting in higher metal dissolution rates and concomitant reduction in conductivity and maybe durability. Thus it would be expedient to pursue options (such as supported metal nanoparticles) that minimize the possibility of metal dissolution.

The propensity for metal nanoparticle oxidation (possibly yielding degradation exacerbating ions) within the PEM in the vicinity of the electrodes as well as the possibility of electronic shorting should be kept in mind. While *ex-situ* post test analysis with tested composite membrane samples suggested that the metal nanoparticles in the PEM did not contribute to Fenton-like catalytic activity, the lower conductivity is observed possibly due

to exchange of protons in sulfonic acid with metal ions formed close to the cathode. Future efforts will be focused on enhancing the efficacy of supported metal nanoparticles in mitigating PEM degradation and designing layered membranes that further negate the impact of possible metal dissolution and electronic shorting. Efforts are also ongoing to delineate the mechanism of degradation mitigation using metal nanoparticles by examining the influence of surface charge on antioxidant activity.

TEM and SEM micrographs

TEM and SEM images of Ag and Au nanoparticles, silica support and Ag, Au, Pd and Pt nanoparticles supported on silica are shown in the Figures S4-S8 below. These figures are representative of the metal and supported metal nanoparticles studied. The dimensions of the support particles were in the range of 100-200 nm, while freestanding metal nanoparticles were approximately 2-5 nm.

The metal nanoparticles supported over silica had larger diameters than unsupported metal nanoparticles as a consequence of the method employed in their synthesis. To produce metal supported over silica nanoparticles, the metal salt was reduced in aqueous solution using citrate in the presence of the support (silica nanoparticles). Citrate acted both as reducing agent and as the stabilizing agent; it adsorbed onto the surface of the nanoparticles and inhibited the deposition of more metal. The interaction of citrate with metal surface was not strong, hence the particles obtained were not as small as the ones obtained using other capping agents.

Free standing metal nanoparticles were prepared using a completely different approach. The reaction was performed using a two-phase mixture and the metal salt was initially

transferred to the organic phase. Then, the reduction was carried out using a strong reducing agent (sodium borohydride) in the presence of dodecanethiol. The sodium borohydride reduced the small amount of metal present in the aqueous phase and once formed, the thiol reacted chemically on the surface of the metal nanoparticle, passivating it and avoiding further particle growth. The dodecanethiol capped nanoparticle was covered by a hydrophobic layer and hence allowed the transfer of the metal nanoparticle to the organic phase, protecting them from side reactions or further growth that could occur in the aqueous phase. After the metal was consumed in the aqueous phase, more metal was transferred from the organic phase and the cycle repeated until all the metal precursor was consumed. This method allowed the preparation of very small nanoparticles. Particles of around 2 nm were obtained using this method.

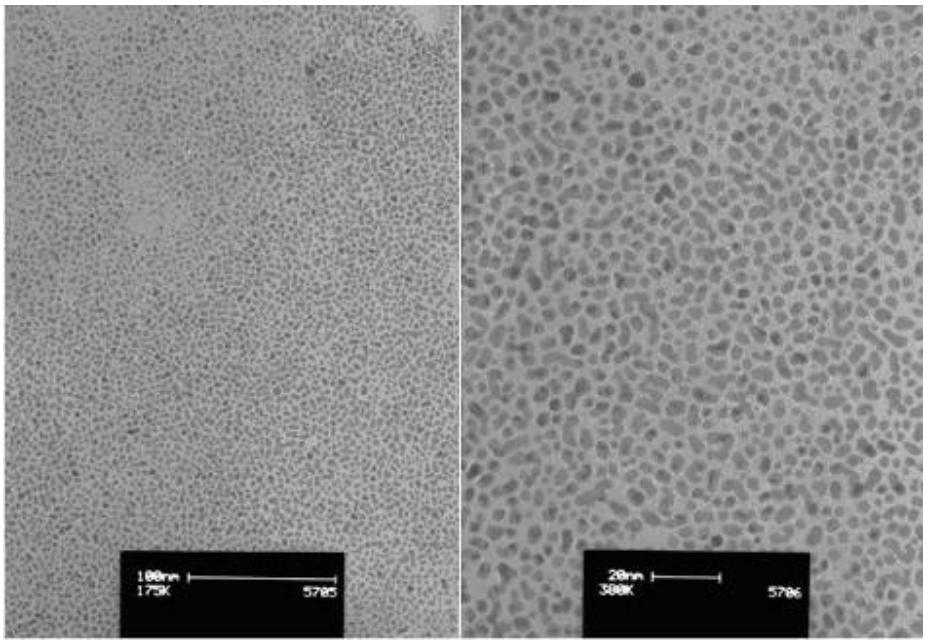

Figure S4. TEM micrographs of Ag and Au nanoparticles.

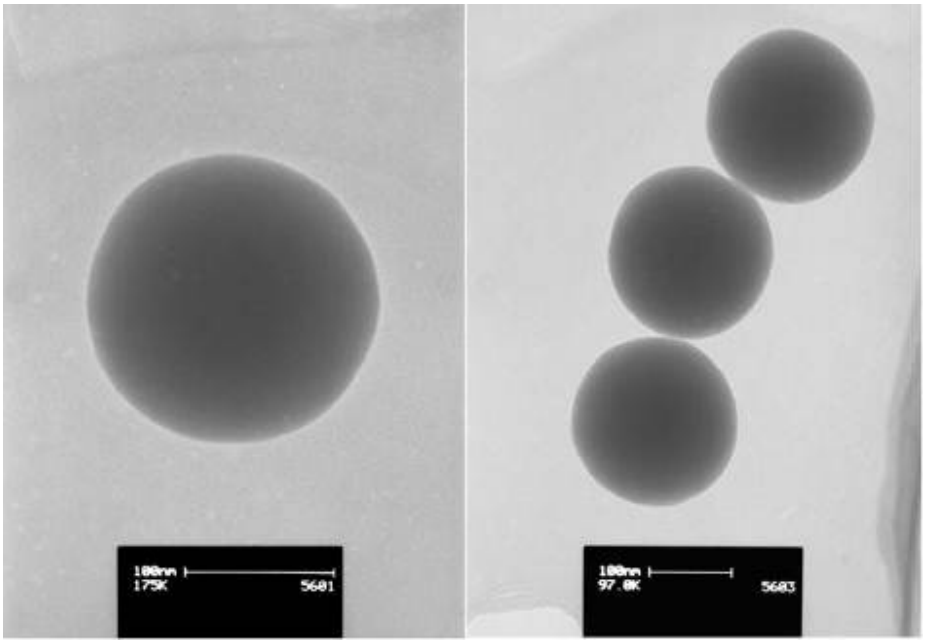

Figure S5. TEM micrographs of SiO_2 support.

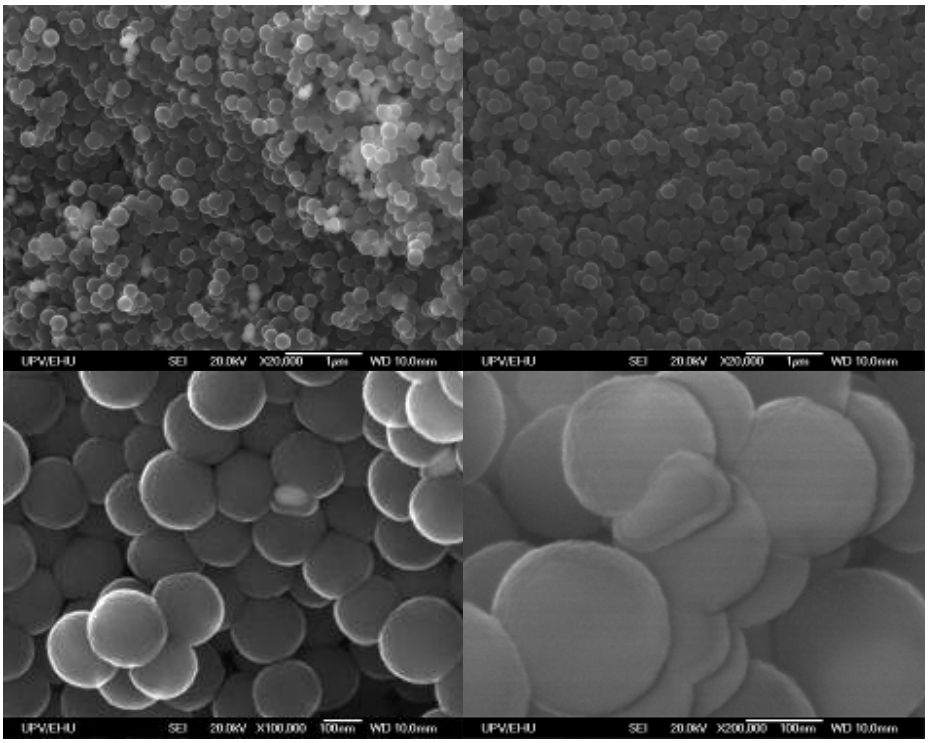

Figure S6. SEM micrographs of SiO_2 support.

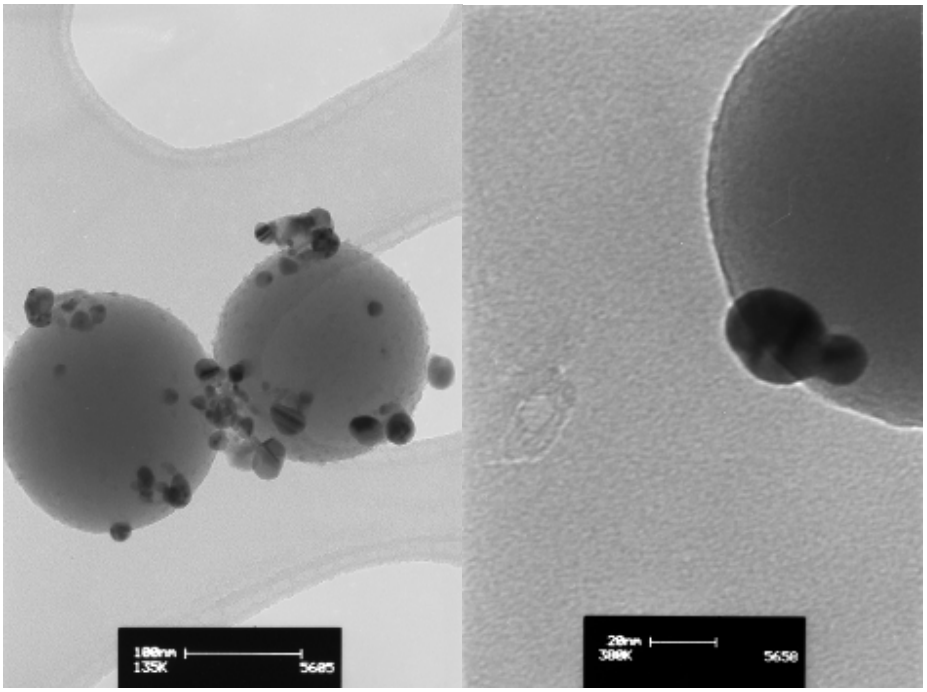

Figure S7. TEM micrographs of Ag and Au supported on SiO_2 nanoparticles.

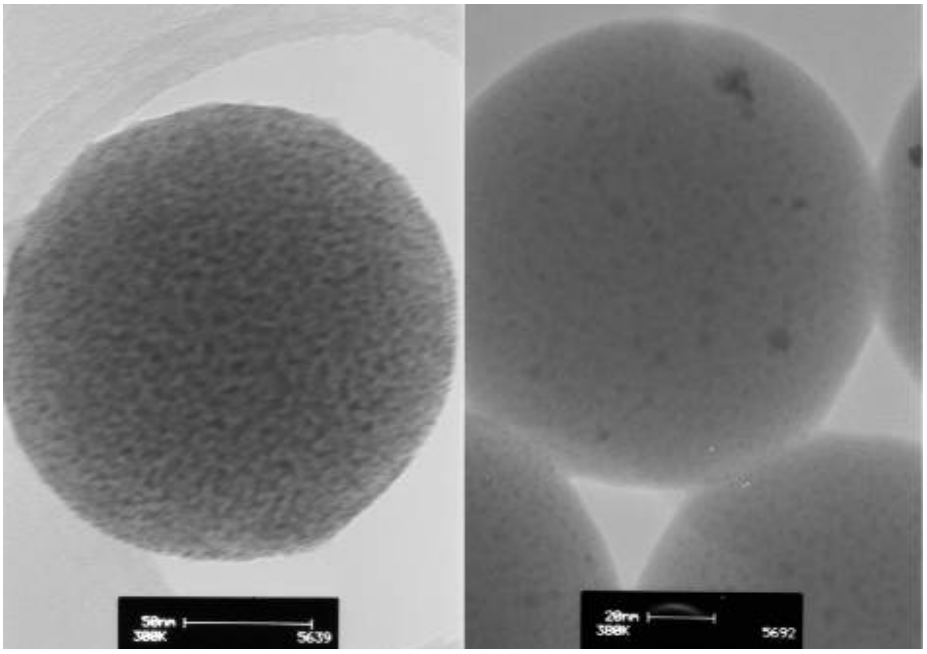

Figure S8. TEM micrographs of Pt and Pd supported on SiO_2 nanoparticles.

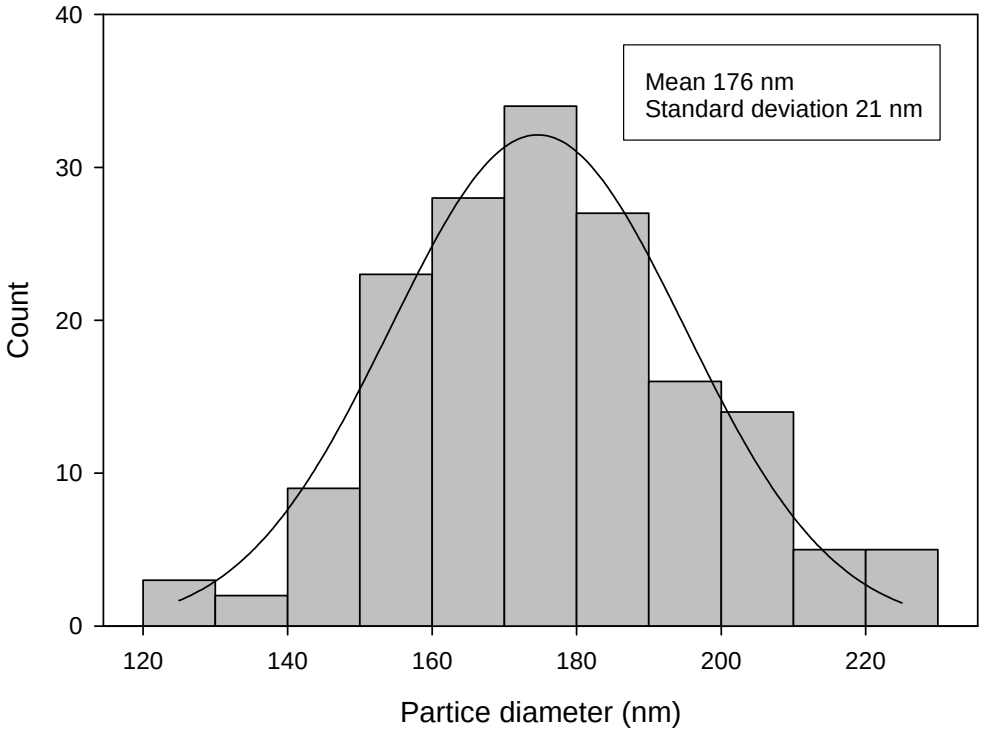

Figure S9. Particle size distribution for the SiO_2 nanoparticles.

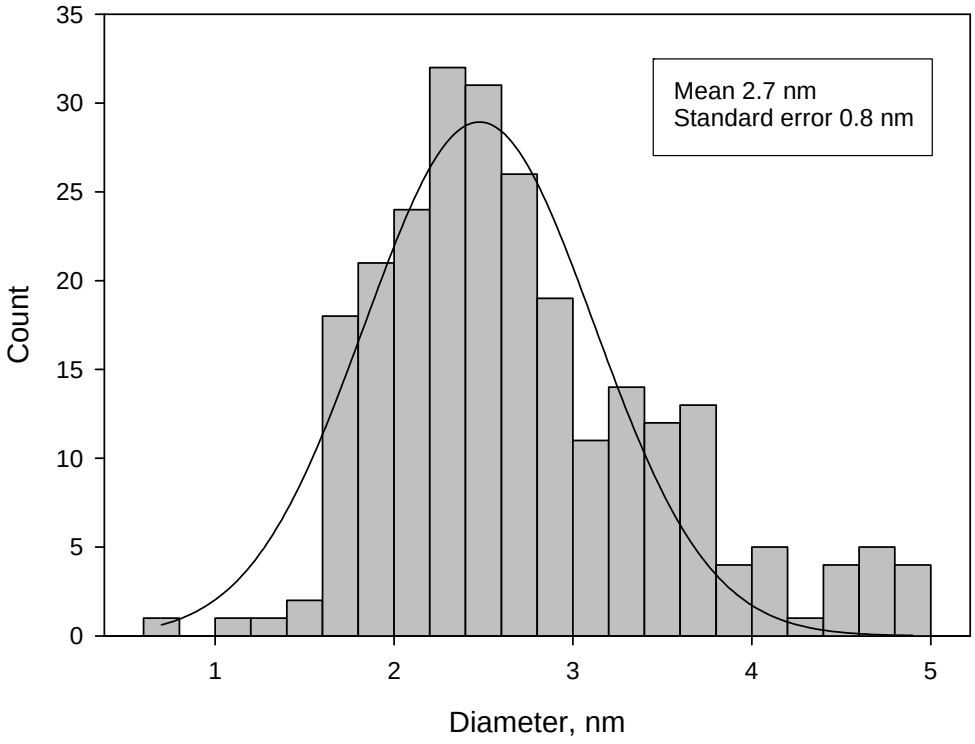

Figure S10. Particle size distribution for the freestanding gold nanoparticles.

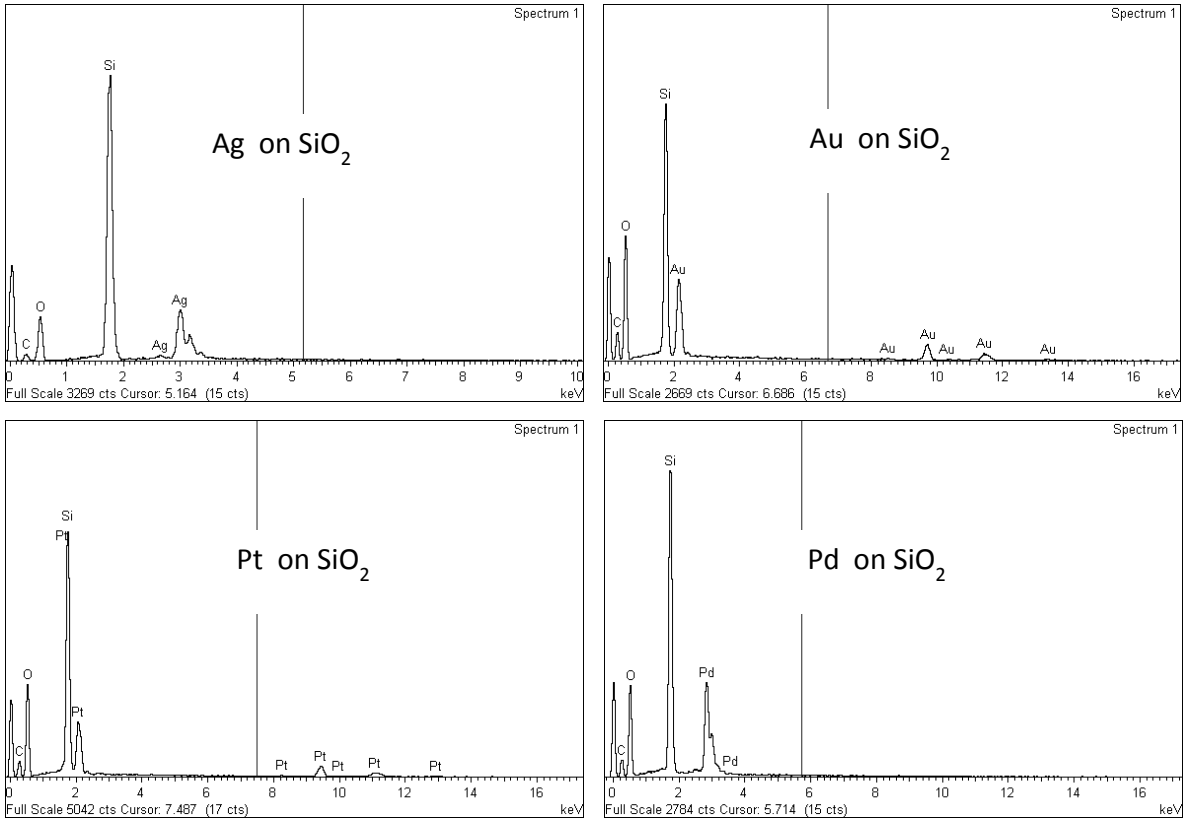

Figure S11. Qualitative EDX analysis demonstrating the presence of metal supported over the silica.

Additional Discussion Items

Work performed in industry has shown clearly that the initial FER correlates directly to stack life, with a strong correlation coefficient. Since the onset of degradation is a process with a long induction period, any added reduction in initial FER can translate into 100s to 1000s of hours or more of improved durability in the stack. The increase in lifetime enabled by the order of magnitude lowering in FER observed in this study is therefore very important and is well worth the additional PEM cost.

References

1. R. Isono, T. Yoshimura and K. Esumi, *J. Colloid Interface Sci.*, 2005, **288**, 177-183.
2. T. Masuda, S. Yonemori, Y. Oyama, Y. Takeda, T. Tanaka, T. Andoh, A. Shinohara and M. Nakata, *J. Agric. Food Chem.*, 1999, **47**, 1749-1754.
3. P. Ionita, *Chem. Pap.*, 2005, **59**, 11-16.
4. K. P. Suja, A. Jayalekshmy and C. Arumughan, *J. Agric. Food Chem.*, 2004, **52**, 912-915.
5. J. Krzystek, A. Sienkiewicz, L. Pardi and L. C. Brunel, *J. Magn. Reson.*, 1997, **125**, 207-211.
6. E. T. Denisov, T. G. Denisova and T. S. Pokidova, *Handbook of Free Radical Initiators*, Wiley Interscience, New Jersey, 2003.
7. G. Strukul, *Catalytic Oxidations with Hydrogen Peroxide as Oxidant*, Springer, New York, 1992.
8. T. Z. Liu, T. F. Lin, D. T. Y. Chiu, K.-J. Tsai and A. Stern, *Free Radical Biol. Med.*, 1997, **23**, 155-161.
9. M. Pourbaix *Atlas of Electrochemical Equilibria in Aqueous Solutions*, Pergamon Press, New York, 1966.
10. W. Liu and D. Zuckerbrod, *J. Electrochem. Soc.*, 2005, **152**, A1165-A1170.
11. S.-Y. Lee, E.-A. Cho, J.-H. Lee, H.-J. Kim, T.-H. Lim, I.-H. Oh and J. Won, *J. Electrochem. Soc.*, 2007, **154**, B194-B200.
12. H. Tang, Z. Qi, M. Ramani and J. F. Elter, *J. Power Sources*, 2006, **158**, 1306-1312.